ARTICLE OPEN

Check for updates

Deciphering autism heterogeneity: a molecular stratification approach in four mouse models

Caroline Gora[1], Ana Dudas[1], Océane Vaugrente[1], Lucile Drobecq[1], Emmanuel Pecnard[1], Gaëlle Lefort[1] and Lucie P. Pellissier[1]✉

Autism spectrum disorder (ASD) is a complex neurodevelopmental condition characterized by impairments in social interaction and communication, as well as restrained or stereotyped behaviors. The inherent heterogeneity within the autism spectrum poses challenges for developing effective pharmacological treatments targeting core features. Successful clinical trials require the identification of robust markers to enable patient stratification. In this study, we identified molecular markers within the oxytocin and immediate early gene families across five interconnected brain structures of the social circuit. We used wild-type and four heterogeneous mouse models, each exhibiting unique autism-like behaviors modeling the autism spectrum. While dysregulations in the oxytocin family were model-specific, immediate early genes displayed widespread alterations, reflecting global changes across the four models. Through integrative analysis, we identified *Egr1*, *Foxp1*, *Homer1a*, *Oxt*, and *Oxtr* as five robust and discriminant molecular markers that allowed the successful stratification of the four models. Importantly, our stratification demonstrated predictive values when challenged with a fifth mouse model or identifying subgroups of mice potentially responsive to oxytocin treatment. Beyond providing insights into oxytocin and immediate early gene mRNA dynamics, this proof-of-concept study represents a significant step toward the potential stratification of individuals with ASD. This work has implications for the success of clinical trials and the development of personalized medicine in autism.

Translational Psychiatry (2024)14:416 ; https://doi.org/10.1038/s41398-024-03113-5

INTRODUCTION

Autism spectrum disorder (ASD) is a heterogeneous neurodevelopmental condition, with a prevalence of 1% [1]. ASD is characterized by impairments in social communication and interaction, as well as repetitive or stereotyped behaviors [2], associated with various co-occurring features. Despite the identification of over thousands of genes associated with ASD, the etiology of most cases remains idiopathic. Early behavioral interventions address social features, but heavily rely on intensive and costly training [3, 4]. Although atypical antipsychotics have gained approval for targeting some co-occurring features, their efficacy is often limited, and they are associated with side effects [5, 6]. To date, clinical trials for drugs specifically targeting core features have encountered setbacks due to their lack of efficacy [7, 8]. The failure of these trials can be attributed to the inherent heterogeneity observed across the spectrum. The success of future trials depends on stratifying this diversity into subgroups within the autism spectrum and identifying reliable markers. Common pathological mechanisms in ASD include global alterations in synaptic activity and plasticity, such as imbalances in GABA and glutamate or reduced oxytocin (OT) levels [9–13]. Among these alterations, meta-analyses of multi-omic studies identify molecular markers such as members of the immediate early genes (IEGs), neurotrophic factors, and components of the OT pathway [14–19].

OT and its paralog vasopressin (AVP), along with their receptors, regulate various social interactions throughout life, including maternal and socio-sexual behaviors [20–23]. These neuropeptides are predominantly synthesized in the somas of OT and AVP neurons located in the paraventricular (PVN) and supraoptic (SON) nuclei of the hypothalamus [24–27]. They project to and release these peptides in response to stimuli in brain structures of the emotional and social circuit, where their receptors are expressed, or in the periphery via the pituitary gland [28–30]. Among these structures, the prefrontal cortex (PFC), and the caudate putamen (CPU) and nucleus accumbens (NAC) of the striatum are interconnected and play a key role in both motor behaviors and social interaction and reward [31–35]. Disruptions in these regions are associated with core autism-like features in mice. There is emerging evidence suggesting a potential link between dysregulation of the OT system and the etiology of ASD (for reviews [36–39]), particularly the association with pathogenic variants in oxytocin (*OXT*), oxytocin receptor (*OXTR*), and vasopressin receptor 1A (*AVPR1A*) genes (SFARI Gene). Additionally, *OXT* mRNAs are particularly susceptible to deadenylation and degradation [19] and both *OXT* and its receptor, *OXTR*, show reduced levels in the brains of individuals with ASD or related conditions [40, 41] and mouse models displaying autism-like behaviors [39, 42]. Notably, deletion of *Oxtr* and *Avpr1a* genes in mice has been shown to induce autism-like behaviors (for review [8]). Nevertheless, the administration of OT has yielded inconsistent effects on social traits in individuals with ASD [8, 43, 44]. Intriguingly, a study has suggested that the concentration of OT in the blood of individuals

[1]INRAE, CNRS, Université de Tours, PRC, 37380 Nouzilly, France. ✉email: lucie.pellissier@inrae.fr

Received: 10 September 2024 Revised: 19 September 2024 Accepted: 23 September 2024
Published online: 04 October 2024

diagnosed with autism could predict the outcome of oxytocin administration [45]. It remains unclear whether mRNAs within this family can serve as shared or specific molecular markers for individuals with ASD.

Multiple studies evidenced global alterations in neuronal activation and synaptic plasticity in ASD [17, 19, 46, 47]. IEGs are rapidly transcribed, and translated within 30 min to 2 h in response to various stimuli, including social interactions [48–50]. Following this initial response, IEGs orchestrate long-term plasticity, notably by initiating the second wave of late genes within 4–24 h for some IEGs that are transcription factors. IEG mRNAs represent key molecular markers of neuronal activation. Dysregulation of their expression has been observed in both plasma and brain tissues of people with ASD [51–55] and animal models mimicking ASD features [56–58]. Whether specific IEGs can serve as predictive markers for distinct autism subtypes remains an open avenue for investigation.

In this study, we used three distinct genetic mouse models—*Shank3*, *Fmr1* and *Oprm1* knockout (KO) mice—alongside mice subjected to early chronic social isolation, encompassing diverse etiologies to model the autism spectrum. Our investigation revealed that each model exhibited a distinctive behavioral signature, mimicking the complexity of the spectrum. We pinpointed *Egr1*, *Foxp1*, *Homer1a, Oxt* and *Oxtr* as robust molecular markers within the OT and IEG gene families. These markers exhibited specific responses to social interactions in wild-type (WT) mice and significant dysregulations in the aforementioned four mouse models across five structures of the social circuit. Using these five markers, we successfully demonstrate the first proof-of-concept for the stratification of mouse models, differentiating subtypes of autism-like behaviors. The identification of these specific markers offers a promising avenue for tailoring personalized medical help to individuals with autism.

MATERIALS AND METHODS

Animals

All mouse breeding, care, and experimental procedures were in accordance with the European and French Directives and approved by the local ethical committee CEEA Val de Loire No. 19 and the French Ministry of Teaching, Research and Innovation (APAFIS #18035-2018121213436249). Mouse models were selected based on their distinct etiologies and behavioral phenotypes, which are well-documented in the literature and consistently observed across laboratories: the mu-opioid receptor deletion—*Oprm1* KO (JAX stock #007559) [59], the synaptic anchoring protein deletion—*Shank3* KO (JAX stock #017688) [32], the X-linked mRNA binding protein deletion—*Fmr1* KO and females *Fmr1*$^{+/-}$ (provided by Rob Willensem [60]) and the IEG deletion—*Arc* KO (JAX stock #007662) [61], modeling ASD genetic cases. Additionally, "isolated" animals exposed to chronic social isolation after weaning for at least 4 weeks prior to behavioral tests were used to mimic idiopathic cases. Animals were maintained on a mixed 50% C57BL/6J—50% 129S2 background. Each mouse line was outcrossed with fresh mixed backgrounds every 5–10 generations, and between these outcrosses, with WT mice from other lines, to prevent inbreeding and ensure consistency among mice across independent batches and lines (Fig. S1). Mice were kept on a regular 12-h light/dark cycle, with food and water available *ad libitum*, at a controlled temperature of 21 °C and 50% humidity in conventional housing conditions. After breeding heterozygous F0 parental mice, 3–4 unrelated WT and KO couples were housed separately to avoid the effects of the social environment [62], and all offspring were raised in social groups of 2–4 individuals per sex for testing. Two months old naive male and female mice were randomly assigned to housing conditions by an experienced experimenter.

Behavior experiments

All behavioral tests were sequentially performed in a dim light quiet room, using standardized equipment, and are detailed in the supplementary methods. Briefly, social interactions were performed in the three-chambered and in reciprocal social interaction tests with a sex- and age-matched unknown mouse or a cage mate in an open field. Non-social interactions were tested with an object also in open field arenas. Perseveration and cognitive flexibility in a spatial task were assessed in the Y-maze test, while repetitive and stereotyped behaviors were examined in the motor stereotypy test, assays that have been previously characterized for mouse models of ASD [63]. While experimenters were not blinded to the conditions during the tests to prevent any mixing of mice, scoring was conducted manually for reciprocal social interaction and three-chambered tests by a trained experimenter who was blinded to the conditions, or automatically for the Y maze and open field tests. All animal research criteria have been reported in accordance with the ARRIVE guidelines [64]. The WT group consisted of distinct batches of WT mice raised in social groups, serving as the respective controls for each mouse line or housing condition and batch.

Quantitative PCR

Mice were dissected at basal conditions or 0.75 (45 min), 2 or 6 h following a social or an object interaction. Within 5 min, 1 mm-thick brain slices were generated using a coronal mouse brain matrix (Vivo-tech Aniphy, VI-68707). Tissue samples of the prefrontal cortex (PFC), nucleus accumbens (NAC), caudate putamen (CPU), paraventricular nucleus (PVN), and supraoptic nucleus (SON), the five brain regions of the social circuit selected for their interconnections and their roles in social interaction impairments and motor stereotypies (anatomical coordinates in Fig. S1E, F) were collected using a 2 mm diameter puncher (with two punches for lateralized regions) and were immediately frozen until further use. After tissue homogenization using a polytron (Grosseron, France, PT1200E), total RNAs were extracted according to the Direct-zol™ RNA Microprep and Miniprep kit (ZymoResearch, Ozyme, France, respectively R2063 and R2050) and quantified using ND2000 nanodrop (Thermofisher, France). The cDNAs were generated from 0.5 or 0.25 µg of total RNAs using the SensiFast reverse transcriptase kit (Ozyme-Bioline, BIO-65054) and quantitative PCR (qPCR) was performed in triplicates according to 2X ONE Green Fast qPCR premix (Ozyme, France, OZYA008-1000) with 1 µL of cDNA and 1 µM of each validated couple of primers (Table S1). The following qPCR protocol was applied for 40 cycles: 95 °C for 5 s, 60 °C for 15 s, and 60 °C for 30 s.

Data modeling and correlations

All statistical analyses were performed using R (version 4.2.2) [65]. Animal outliers (±3 standard deviations) were removed. Variability between cohorts (Fig. S1) was assessed using Principal Component Analysis (PCA) with the FactoMineR package [66]. For qPCR, batch corrections were applied using the ComBat sva package [67] (Fig. S1A–C), while the behavior across the distinct WT batches remained consistent and did not require correction (Fig. S1D). For behavioral data and OT peptide levels, Kruskal-Wallis tests with Dunn's post hoc tests were conducted using the rstatix package [68]. *P*-values were adjusted with Benjamini–Hochberg correction [69]. A complete linear model was fitted for qPCR data and IEG protein levels, encompassing variables such as time, social interaction, or mouse line, and their interactions. Post-hoc tests, based on estimated marginal means with Sidak *p*-value correction, were conducted using the emmeans package [70] to compare social interaction at each time point, the different time points for each interaction, and mouse models to WT mice. In addition, the analyses were conducted separately as PCA revealed distinct clusters among the structures: one comprising PFC, NAC, and CPU, and the other involving PVN and SON (Fig. S1C). Sex differences in behavioral and qPCR data were analyzed only in WT mice, as sample sizes for the other mouse models were too small for comparison. In WT mice, clustering of genes and median expressions was performed using the pheatmap package. Furthermore, the integration of qPCR and behavioral data was performed using DIABLO (Multiblock (s)PLS-DA) implemented in the mixOmics package [71, 72]. The compromise parameter was set at 0.75 to maximize the correlation between qPCR and behavioral datasets. Linear discriminant analysis (LDA) was performed using *Egr1*, *Foxp1*, *Homer1a, Oxt* and *Oxtr*, on each mouse with less than 5 missing values across all structures, using the MASS package [73]. LDA predicted the class membership of *Arc* KO mice that were not considered during model fitting (i.e., the model with most similarities). Finally, on the data of *Shank3* and *Fmr1* KO mice and only on the OT markers, hierarchical clustering on the principal components of PCA (HCPC) was performed using the FactoMineR package [66].

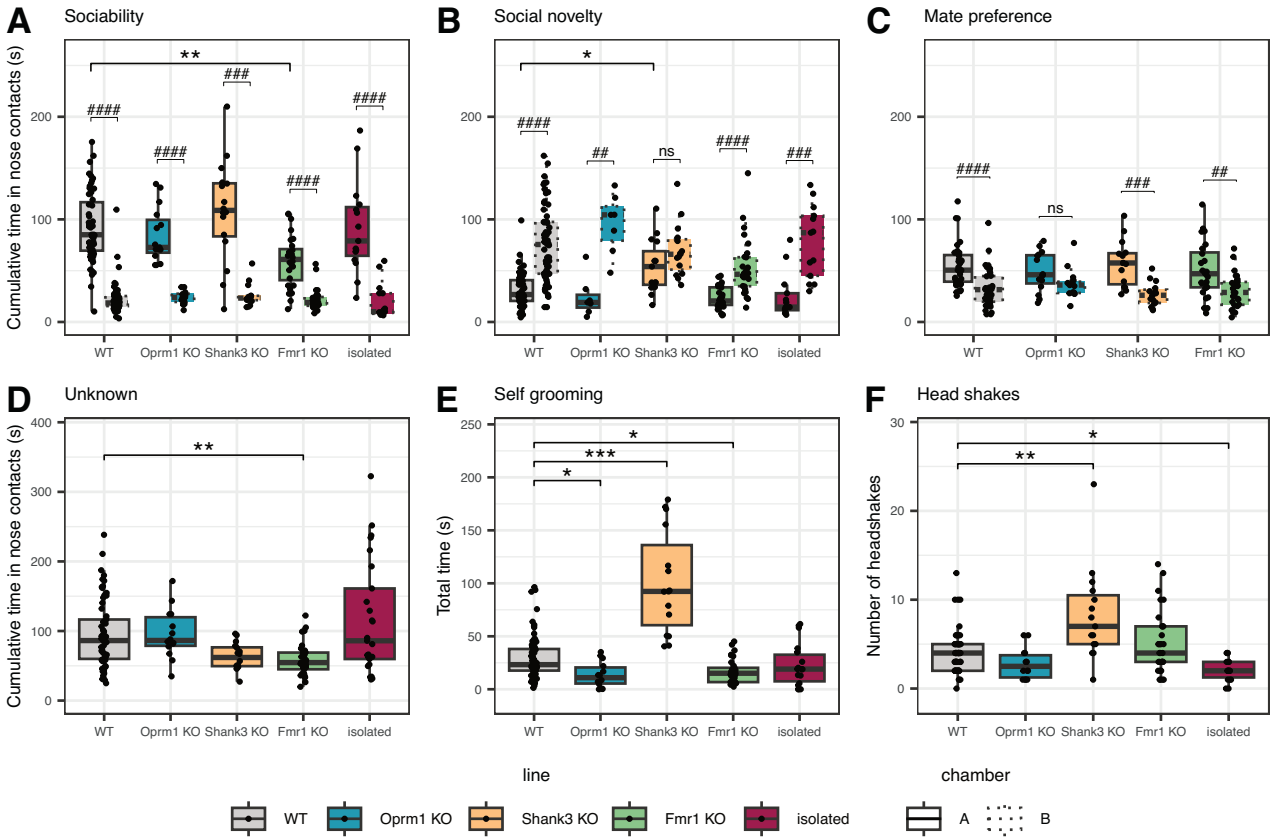

Fig. 1 All four models exhibited distinct behavioral features along the autism spectrum. In the sociability (**A**), the social novelty (**B**) or mate preference (**C**) phases of the three-chambered test, the cumulative time in nose contacts of *Oprm1, Fmr1, Shank3* KO and isolated mice are compared to WT animals. In the sociability phase, *Fmr1* KO mice exhibit reduced time spent in nose contact with an unknown WT mouse (chamber A) compared to WT mice, but not with the object (chamber B). In the social novelty phase, *Shank3* KO mice display no preference for the novel mice (unknown WT mouse, chamber B) over the familiar mouse (already explored for 10 min in the precedent phase, chamber A). *Oprm1* KO mice show a lack of preference for the cage mate (chamber A) over the familiar mouse (already explored for 10 min in the precedent phase, chamber B). In the reciprocal social interaction tests, the cumulative time in nose contacts with a genotype-, sex- and age-matched unknown mouse (**D**) is reduced in *Fmr1* KO mice (green), but not in *Oprm1* (blue), *Shank3* KO (yellow) and isolated (burgundy) mice, compared to WT animals (gray). In motor stereotypies, the time spent in self-grooming (**E**) is increased in *Shank3* KO mice and reduced in *Oprm1* and *Fmr1* KO animals, while the number of head shakes (**F**) is increased in *Shank3* KO mice and reduced in isolated mice, compared to WT mice. Data are presented as individual data, mean ± sd (Table S2). Kruskal–Wallis tests followed by Dunn *post hoc* tests were performed with stars as line effect and hash as chamber effect (p = adjusted p-value with Benjamini–Hochberg correction). * or # $p < 0.05$, ** or ## $p < 0.01$, *** or ### $p < 0.001$, **** or #### $p < 0.0001$.

RESULTS

Distinct behavioral profiles across autism spectrum in four mouse models

We examined the behavioral profiles of *Fmr1* and *Shank3* KO mice, modeling Fragile X and Phelan–McDermid syndromes, respectively, along with *Oprm1* KO and chronically isolated mice (Fig. 1, S2–S4, Table S2), all previously published as mouse models displaying autism-like and neurodevelopmental conditions [32, 74–76]. To capture a comprehensive view of their social responses, we exposed these models to distinct social interactions: one involving a family member (e.g. a cage mate, "SI mate") and the other with an unknown conspecific ("SI unknown"), mimicking the daily life of individuals with autism. Additionally, we included a non-social interaction condition with an object ("NSI object"), as control.

In the open field, none of the models exhibited altered behavior following SI mate or NSI object (Table S2). *Fmr1* KO mice demonstrated robust social impairments, indicated by a decrease in both total time and mean duration engaged in nose contacts with an unknown mouse both in the reciprocal and three-chambered tests (Fig. 1A, D). This impairment was also observed in heterozygous females in the sociability phase of the three-chambered test (Fig. S2A–C). In contrast, *Shank3* KO mice displayed impaired social novelty, evident in their lack of preference for a new mouse over a familiar one (Fig. 1B). Surprisingly, *Oprm1* KO and isolated mice did not exhibit the expected social impairments as reported previously [74, 76]. Under standard conditions, *Oprm1* KO mice only displayed a lack of mate preference in the three-chambered test (Fig. 1C). Elevating light intensity from 15 to 40 lx to strengthen anxious-like behavior revealed social interaction impairments with an unknown animal in *Oprm1* KO mice, as evidenced by a reduction in the time spent in nose contact during both the sociability and social novelty phase of the three-chambered tests, as opposed to WT mice tested in dim light conditions (Fig. S2D–F). Additionally, sex effect analyses indicated that WT males exhibited increased time in nose contact during the social novelty phase of the three-chamber test (Fig. S3A–D). This finding suggests a potential manifestation of induced social impairments or social anxiety—a phenotype situated at the periphery of the autism spectrum.

Regarding stereotyped behaviors, *Shank3* KO mice spent more time in self-grooming, accompanied by an increased number of head shakes and a decrease in the time spent digging and in the

number of rearing events compared to WT mice (Fig. 1E, F, S4A, B). Conversely, *Oprm1* and *Fmr1* KO mice demonstrated a reduction in self-grooming time, while isolated mice exhibited a decreased number of head shakes (Fig. 1E, F). WT males displayed a higher number of head shakes compared to females (Fig. S3A–D). Concerning co-occurring features, none of the models exhibited impaired cognitive flexibility in the Y maze, nor did they show locomotion impairments in the open field (Fig. S4C, D). Notably, *Shank3* KO mice displayed anxious-like behaviors, spending more time in the periphery of the open field arena compared to WT mice (Fig. S4E).

In summary, the four models presented distinct behavioral features modeling the autism spectrum, with *Fmr1* and *Shank3* KO mice displaying the most severe phenotypes.

Identification of specific molecular markers of social interactions in WT mice

Given that molecular markers for social interactions remain unknown, our primary objective was to identify them, starting with WT mice. We focused on two mRNA families, recognized as potential molecular markers of autism [8, 17, 39, 77]: the OT family, encompassing *Oxt* and *Avp*, and their receptors (*Oxtr*, *Avpr1a*, *Avpr1b*), and IEGs and neurotrophic factors, including *Arc*, *Egr1*, *Fos, Fosb, Jun*, *Homer1a*, *Foxp1, Gdnf* and *Bdnf*. We investigated their kinetic profiles up to 6 h after SI mate, SI unknown, and NSI object, as well as 6 h following acute social isolation, a condition with negative social valence. We studied their profiles across five key structures within the social circuit: the paraventricular (PVN) and supraoptic nuclei (SON) of the hypothalamus, the caudate putamen (CPU) and nucleus accumbens (NAC) of the striatum, and the medial prefrontal cortex (PFC). To ensure the specificity of our findings, we ruled out circadian or sex biases within the two mRNA families (Fig. S5A, Table S3). Notably, none of these mRNAs displayed distinct patterns within a 6-h period or between males and females, except for *Foxp1*, which exhibited sexually dimorphic expression in the SON. Interestingly, *Arc* in the SON was the only mRNAs down-regulated by acute social isolation from cage mates (Fig. S5B).

Social criteria for selecting mRNAs included a significant regulation following SI unknown or SI mate, and distinct differences from NSI object in at least two separate brain structures (Figs. S6–S8). Consequently, we identified *Oxt* and *Oxtr* mRNAs within the OT family, along with *Foxp1* and *Homer1a* within the IEG family, which were induced by the NSI object in no more than one (and distinct) structure. Among these, *Oxtr* mRNAs emerged as the most reliable marker, showing no induction in response to the NSI object and meeting the social criteria across three different brain structures. Notably, SI unknown at 45 min emerged as the most distinct stimulus with a rapid and transient increase in mRNAs at 45 min, such as *Oxtr* expression in the NAC and CPU and *Homer1a* in the PVN, or conversely, no IEG induction, compared to SI mate and NSI object (Fig. 2A, S6–S8, Table S3). When distinct from NSI object, SI mate induced sustained regulations, like *Foxp1* mRNAs in the PFC. Although the NAC and SON exhibited the highest number of regulations, no single structure or mRNA distinctly stood out for a particular social stimulus, except for *Oxtr*, which was induced following SI unknown and not SI mate (Fig. 2A and S6–S8). Interestingly, SI unknown regulated most IEGs in the PVN and SON (Fig. S8), suggesting potential active processes of social plasticity induction. Remarkably, our datasets in WT and models revealed robust correlations between mRNAs, such as a 0.92 positive correlation between *Oxt* and *Avp* (Fig. S9A, B). Noteworthy, *Foxp1*, *Homer1a* and *Egr1* displayed a negative correlation with *Oxt* and *Avp* (Fig. S9C), suggesting a potential interplay between them.

In summary, we identified *Foxp1*, *Homer1a, Oxt* and *Oxtr* as specific molecular markers of social interactions in WT mice. These markers were selected to assess their levels in the four mouse models, both under basal conditions and following SI unknown at 45 min—the most discriminant interaction and time point.

Distinct dysregulations within the oxytocin family among mouse models

Previous studies have proposed OT, AVP, or their receptors as potential common biomarkers of autism [8, 39, 77]. To explore shared dysregulations within the OT family, using *Oprm1, Fmr1*, *Shank3* KO and isolated mice, we assessed alterations in *Oxt*, *Avp, Oxtr* and *Avpr1a* expression following SI unknown at 45 min and under basal conditions (Figs. 2B, 3A, S10–S12, Table S4). These mRNAs are largely clustered together, separating *Oprm1* KO mice and WT under basal conditions from *Fmr1* KO mice under basal conditions and isolated mice (Fig. 2B). Additionally, we identified shared dysregulations across at least two models—*Avp* in the CPU, *Avpr1a* in the SON and *Oxt* in the NAC (Figs. S10, S11). However, the majority of dysregulations were rather specific for each mouse model. *Fmr1* KO mice displayed a global decrease in the expression of all four mRNAs in the PVN, along with *Avp*, *Oxt*, *Oxtr* in the NAC, and *Oxt* and *Avpr1a* in the SON (Figs. 3A, S10, S11). In contrast, isolated mice exhibited an overall increase in *Avp, Oxt* and *Oxtr* expression in the PFC (Fig. 3A). *Shank3* KO mice did not show additional dysregulations, while in the CPU, *Oxt* and *Avpr1a* were also down-regulated in *Oprm1* KO mice (Fig. S10).

To explore the potential for shared dysregulations beyond the initial OT family, we extended our assessment to include *Cd38*, involved in OT secretion, and *Avpr1b*, along with generalist enzymes involved in peptide biosynthesis (*Pcsk1, Pcsk2, Pcsk5* and *Cpe*) and degradation (*Lnpep*, *Ctsa* and *Rnpep*; Fig. S12, Table S4). Strikingly, only three shared dysregulations—*Cpe*, *Ctsa*, *Rnpep* in the NAC—were observed among the two models (Fig. S12). Once again, the majority of dysregulations demonstrated model specificity. In addition to the shared dysregulations, *Fmr1* KO mice exhibited six unique down-regulations, particularly in the NAC and PVN. Isolated mice displayed mostly up-regulations in the PVN and PFC, along with up- and down-regulations in other structures. *Shank3* KO mice showed a down-regulation of *Cd38* in the NAC and PFC. Notably, none of these mRNAs were affected in *Oprm1* KO mice. To identify the most discriminant mRNAs for model stratification, we applied stringent criteria, requiring a minimum of 6 total and 4 unique dysregulations across three structures and three models. Within the OT family, only *Oxt, Avp* and *Oxtr* met these criteria, spanning four structures and four models (Figs. S10–S12). We assessed the impact of these dysregulations on OT peptide levels in *Fmr1* KO, *Shank3* KO and isolated mice that shared mRNA dysregulations. Although OT concentrations were higher in the PVN as expected and variable between cohorts, no difference was observed in the models compared to their respective WT (Fig. S13A). Plasma OT concentration and urine levels were not correlated with brain concentrations, including PVN and SON (Fig. S13B).

In conclusion, *Oxt*, *Avp* and *Oxtr* emerge as the most discriminant markers within the OT family among the four models. These findings highlight their potential utility in stratifying mouse models based on their unique molecular signatures, rather than revealing shared mechanisms.

Widespread dysregulations in IEG expression across mouse models

Akin to the OT family, we investigated dysregulations in *Arc*, *Egr1, Fos*, *Foxp1* and *Homer1a* across the four models following SI unknown at 45 min and under basal conditions. Our results revealed extensive dysregulations in IEGs across all five structures and mouse models (Figs. 2B, 3B, S14–S15, Table S4). However, the underlying causes of these dysregulations varied among the mouse models (Fig. 2B). In the PVN and SON, IEGs remained at basal levels following SI unknown in *Oprm1* KO mice clustering with WT under basal conditions, while in the other models, IEGs

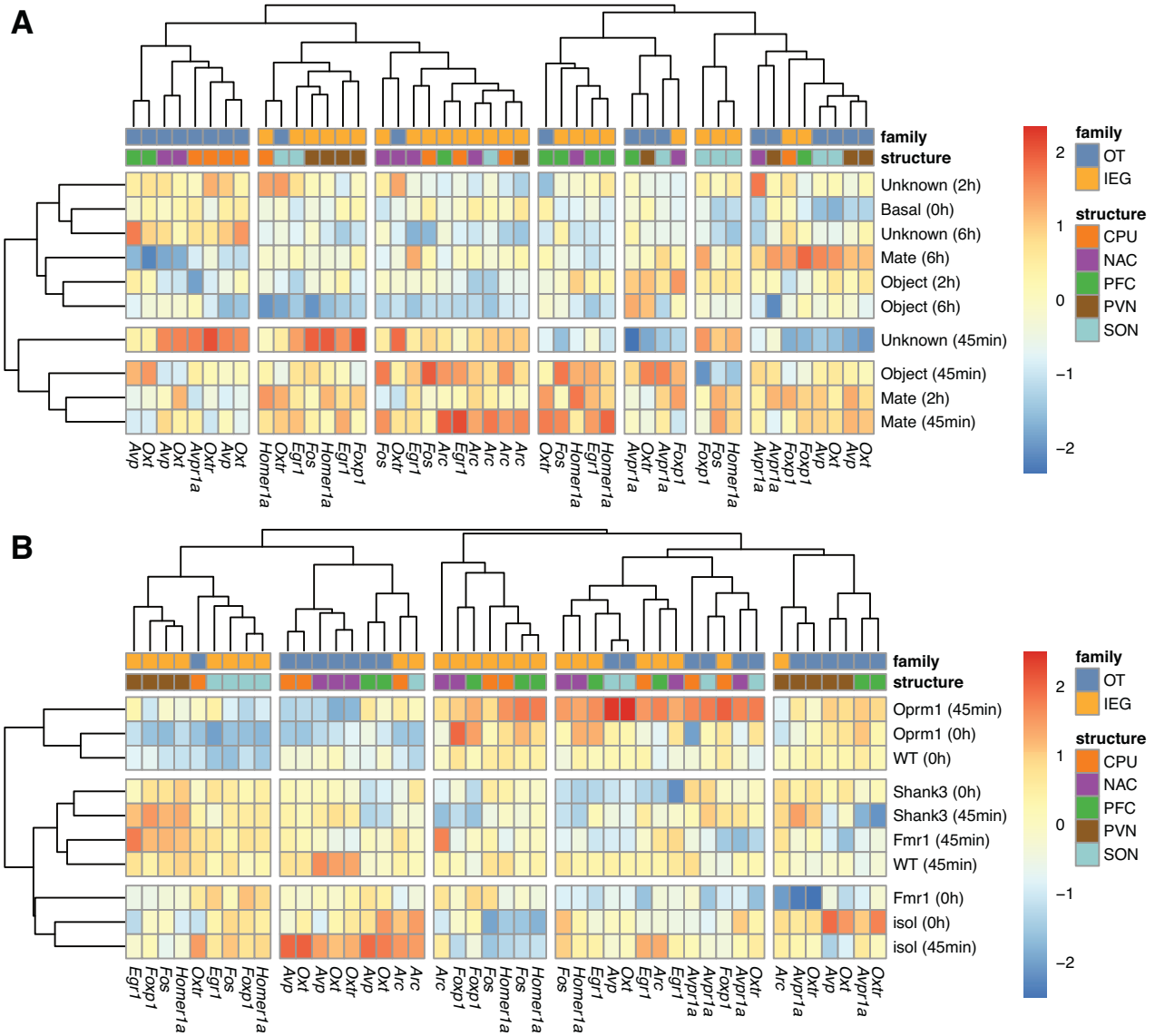

Fig. 2 ***Egr1, Foxp1, Homer1a, Oxt* and *Oxtr* are the most discriminant mRNAs in WT mice and models with ASD-like features.** Hierarchical clustering of the OT (blue) and IEG (orange) mRNAs under basal conditions and 45 min, 2 or 6 h following interactions with an unknown mouse (SI unknown), a cage mate (SI mate) or an object (NSI object) in WT animals **A** identifies three clusters among the different interactions and time points: one cluster with SI unknown at 45 min, one with SI mate at 45 min, 2 h and NSI object at 45 min, and one cluster with the other conditions. mRNAs and structures were separated in 7 clusters (1 to 7 from left to right). Clusters 1 and 2 mainly discriminate mRNAs induced by SI unknown at 45 min in the OT family in the NAC, CPU and PFC and IEGs in the PVN and SON, respectively. Clusters 4 and 7 highlight mRNAs that are not induced by SI unknown at 45 min compared to NSI object and SI mate, while cluster 6 shows the mRNAs that are induced by both social stimuli. Clusters 3 and 5 represent mRNAs induced by SI mate and NSI object or NSI object, respectively. Hierarchical clustering under basal conditions and following SI unknown at 45 min in *Oprm1, Fmr1, Shank3* KO, isolated and WT animals **B** reveals that *Oprm1* KO mice clustered with WT under basal conditions, where IEGs were not induced in the PVN and SON (cluster 1) but were upregulated in other brain regions (clusters 3–4). In contrast, *Fmr1* KO mice at basal conditions clustered with isolated mice, showing upregulation of the OT family and Arc (cluster 2) and lower IEG expression (cluster 3) in the NAC, CPU, and PFC. Following SI unknown, *Fmr1* KO mice clustered with *Shank3* KO mice and WT exposed to SI unknown at 45 min, marked by higher levels of IEGs in the PVN and SON (cluster 1). Blue and red indicate low and high expression levels, respectively. All data, mean and statistical values are represented in Figs. S6–S8, S10, S11, S14, S15 and Tables S3, S4. CPU, caudate putamen; NAC nucleus accumbens, PFC prefrontal cortex, PVN paraventricular nucleus, SON supraoptic nucleus.

were already induced under basal conditions compared to WT mice (Figs. 2B, 3B). Conversely, in the CPU and PFC, the opposite trend was observed (Figs. S14, S15). Clustering separated *Fmr1* KO mice under basal conditions and isolated mice (lower IEG expression in the NAC, CPU, and PFC) from WT and *Fmr1* KO mice following SI unknown at 45 min and *Shank3* KO mice (upregulation of IEGs in the PVN and SON; Fig. 2B). Surprisingly, *Arc* was the only IEG that was frequently clustered with the OT family (Fig. 2B). We identified 6 shared dysregulations in all four models (SON: *Fos*, *Foxp1* and *Homer1a*; PVN, *Egr1* and *Homer1a*; CPU: *Foxp1*), as well as four additional dysregulations in three models (SON: *Egr1*; PFC: *Homer1a*; NAC: *Fos*; CPU: *Homer1a;* Figs. 3B, S14, S15). Applying the same criteria as the OT family, we identified *Egr1*, *Fos, Foxp1* and *Homer1a*, with *Homer1a* standing out with 16 total and 7 unique dysregulations across all five structures and all four models.

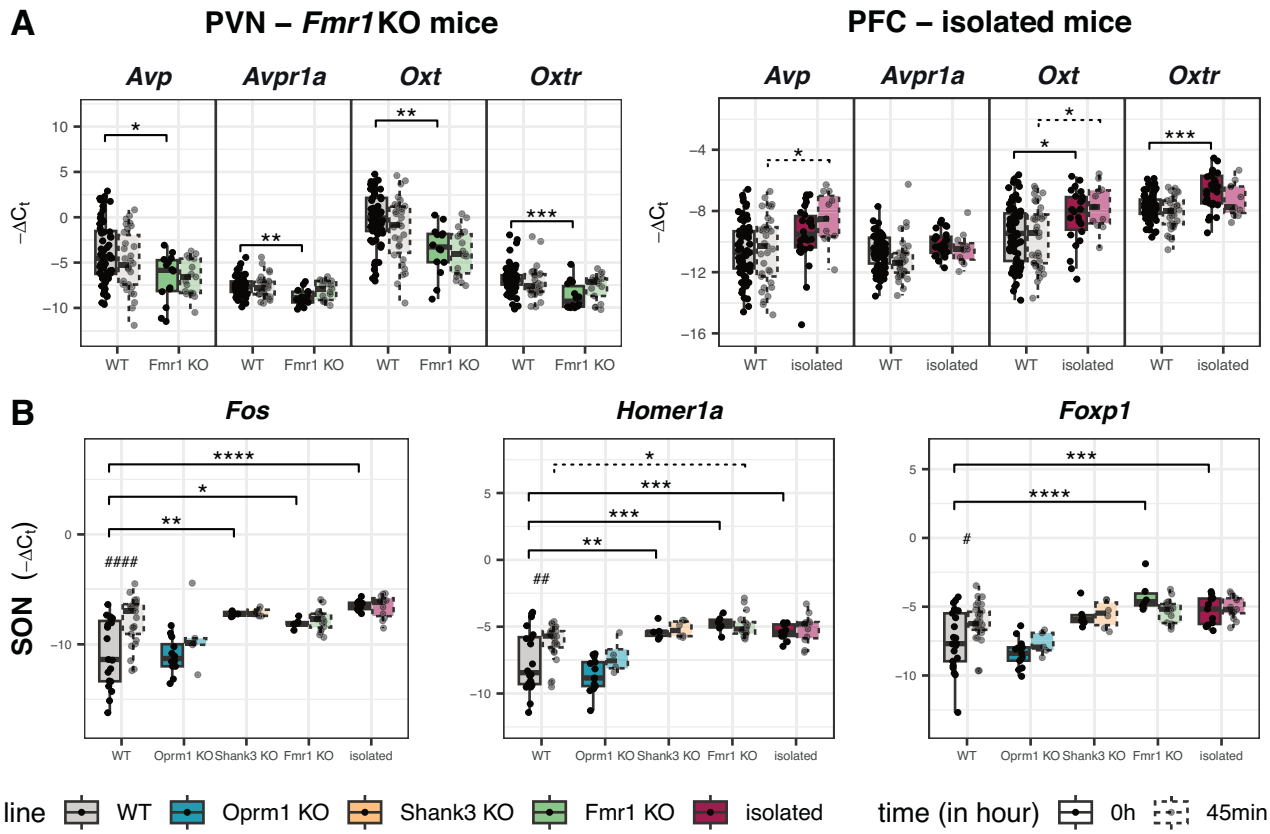

Fig. 3 Dysregulations are model-specific for the OT family and widespread across models for IEGs. Dysregulations in the OT family are rather specific to a model when comparing induced 45 min after social interaction with an unknown mouse (SI unknown, dashed lines) over basal conditions (solid lines) in *Oprm1* (blue), *Shank3* KO (yellow), *Fmr1* KO (green) and isolated (burgundy) mice, compared to WT mice (gray). In the PVN (**A**), *Fmr1* KO mice exhibit reduced levels of *Oxt, Avp, Oxtr* and *Avpr1a* mRNAs under basal conditions, compared to WT mice, while in the PFC, *Avp, Oxt* and *Oxtr* mRNAs are up-regulated in isolated mice (burgundy), compared to WT mice. In the SON, among the IEGs (**B**), *Fos, Foxp1* and *Homer1a* levels were not induced 45 min after SI unknown over basal conditions across the four mouse models for different reasons in these models. While they remained at basal levels following SI unknown in *Oprm1* KO mice, they were already induced under basal conditions in the other three models. Data are presented as individual data, mean ± sd (Table S4). Linear models followed by *post hoc* tests based on estimated marginal means were performed with stars as line effect and hash as basal *vs* SI unknown 45 min effect (p = adjusted p-value with Tukey correction). * or #$p < 0.05$, ** or ##$p < 0.01$, *** or ###$p < 0.001$. PFC prefrontal cortex, PVN paraventricular nucleus, SON supraoptic nucleus.

We evaluated the protein levels of Arc, c-Fos, FoxP1 and Egr1 in basal conditions and two hours after SI unknown in *Fmr1* KO and *Shank3* KO mice, the two models with the most dysregulations (Fig. S16). Although IEG proteins are also dysregulated, particularly in the PVN of *Shank3* KO mice and the NAC of *Fmr1* KO mice, mRNA and protein levels did not match each other (Figs. S14–S16). However, c-Fos protein and *Fos* mRNAs were upregulated following SI or in basal conditions, respectively, in the PVN of *Shank3* KO mice. Interestingly, *FoxP1* mRNAs were reduced while protein was higher in basal conditions in the CPU of *Fmr1* KO mice (Fig. S16), suggesting potential active translation processes and mRNA degradations.

In conclusion, our study unveils widespread dysregulations in IEGs levels across the models. *Egr1*, *Fos, Foxp1* and *Homer1a* emerge as the most dysregulated IEGs in the four mouse models, providing valuable markers for model stratification.

Molecular stratification of mouse models using *Egr1, Foxp1, Homer1a, Oxt* and *Oxtr*

The integration of SI unknown and qPCR data across the four mouse models aimed to link mRNA expression 45 min after SI unknown with specific models and behavioral parameters (Fig. S17). In component 1 (isolated vs. *Oprm1* KO mice), the analysis unveiled a positive association between *Foxp1* in the SON of isolated mice and their increased nose contacts, which negatively correlated with *Oprm1* KO mice (PFC: *Fos* and *Homer1a*) and their increased rearing events (Figs. S17A, B and S18). Additionally, Component 2 identified a positive association between grooming behavior and *Shank3* KO mice, which negatively correlated with *Oxt*, *Avp* and *Oxtr* in the PFC (Figs. S17C and S18). These findings suggest a connection between *Avp*, *Fos, Foxp1, Homer1a, Oxt* and *Oxtr* and core autism-like features in specific models and confirmed the opposition between spatial exploration and social interaction.

Finally, we crossed all our previous conclusions from WT mice and the four mouse models, identifying *Egr1*, *Foxp1, Homer1a*, *Oxt* and *Oxtr*, as the most consistent mRNAs. *Avp* was excluded due to its high correlation with *Oxt* that could bias the model towards their shared dysregulations. Employing these five robust molecular markers, we conducted a proof-of-concept for potential stratification among the four mouse models (Fig. 4). The linear discriminant analysis (LDA) integrated molecular data from these markers across the five brain structures in the four models under basal conditions and following SI unknown (Figs. 4A, B, S18). The analysis unveiled distinct classifications, identifying *Oprm1* KO (LD1) and isolated mice (LD2) as separate models, while the model positioned WT mice in the middle of the four models, as expected. Although *Shank3* and *Fmr1* KO mice clustered together, they exhibited individual characteristics (LD3). Among the markers, LDA coefficients revealed that levels of *Oxt* (LD1–3) and *Homer1a* in the

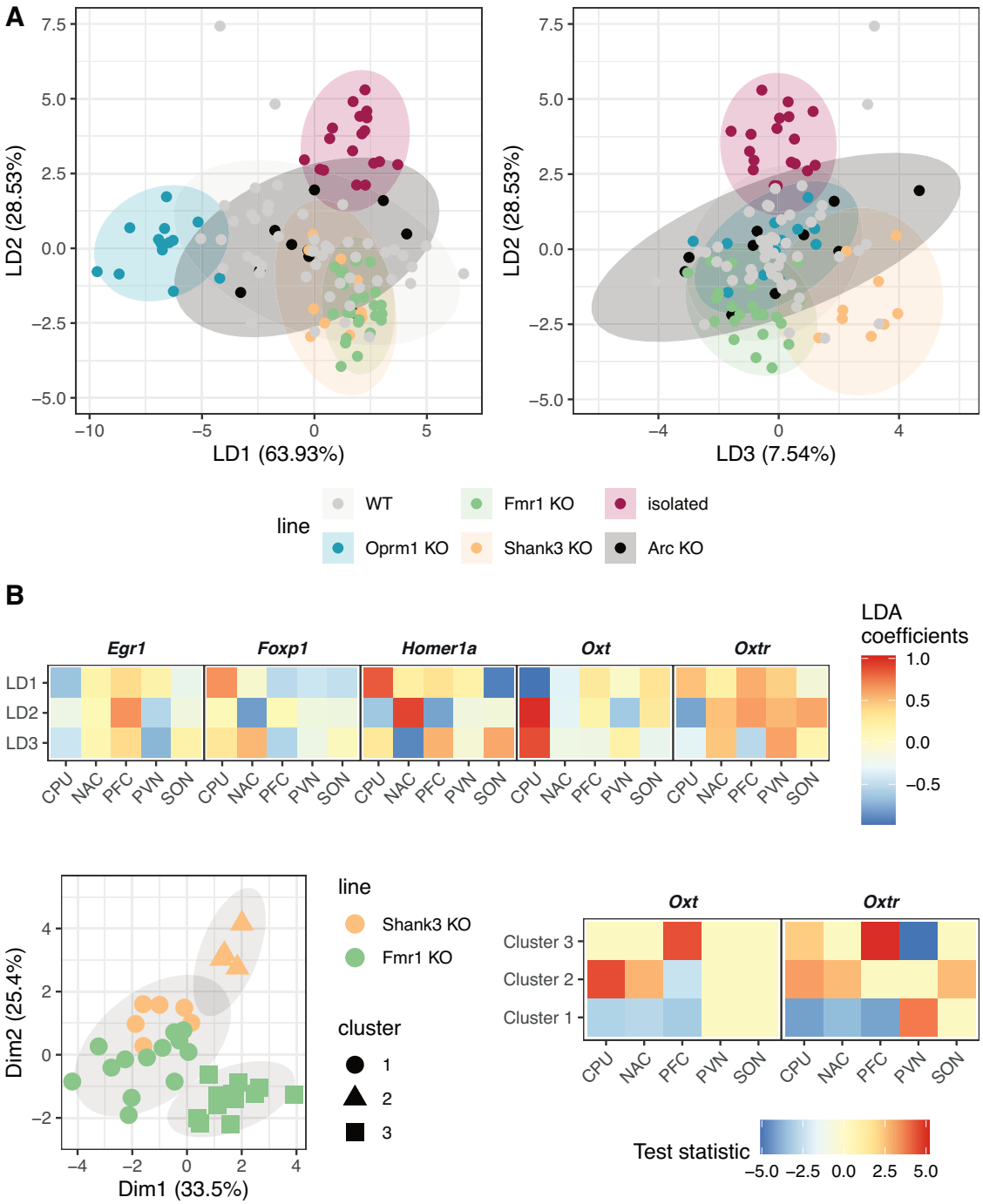

Fig. 4 Stratification of the four models using the five molecular markers *Egr1, Foxp1, Homer1a, Oxt* and *Oxtr*. Linear discriminant analysis (LDA; **A**) revealed that *Oprm1* (blue, LD1 component) and isolated (burgundy; LD2 component) mice clustered apart from the other two models. LD3 component discriminates between *Shank3* KO (yellow) and *Fmr1* KO (green) mice. While challenged with WT (gray) and *Arc* KO mice (black), the stratification predicted that both mice were similar to *Fmr1* KO mice, followed by *Oprm1* KO mice for WT mice and *Shank3* KO mice for *Arc* KO mice. The heatmap with LDA coefficients (**B**) indicates that the five molecular markers, *Egr1, Foxp1, Homer1a, Oxt* and *Oxtr*, contributed to the stratification of the models. Hierarchical Clustering on Principal Components (HCPC; **C**) revealed three subgroups among *Shank3* KO and *Fmr1* KO mice (left panel). Cluster 1, which contains *Shank3* KO and *Fmr1* KO mice, displays lower levels of *Oxt* and *Oxtr* in the CPU, NAC and PFC, as well as increased levels of *Oxtr* in the PVN. Blue, red and white indicate low, high levels or no significant contribution, respectively. PFC prefrontal cortex, NAC nucleus accumbens, CPU caudate putamen, PVN paraventricular nucleus, SON supraoptic nucleus.

CPU and SON (LD1), as well as *Homer1a* in the NAC (LD2–3) exerted the most significant influence on the stratification, followed by *Oxtr* across the structures.

To challenge our stratification, we tested WT and *Arc* KO mice, previously documented to manifest social interaction impairments [61, 78]. Based on the five markers, LDA predicted that WT and *Arc* KO mice would be the closest to *Fmr1* KO mice (with class membership probability of 57 and 60%, respectively), followed by *Oprm1* KO mice (18%), isolated mice (14%) and *Shank3* KO mice (10%) for WT mice and *Shank3* KO mice (20%) and *Oprm1* KO and isolated mice (10%) for *Arc* KO mice (Fig. 4A). Indeed, *Arc* KO mice displayed an intermediate phenotype between *Fmr1* and *Shank3*

KO mice, showing social interaction impairments coupled with increased self-grooming (Fig. S19), further confirming their relevance as a mouse model with ASD-like features. Additionally, we employed our stratification to predict the potential responsiveness of subgroups (e.g., *Fmr1* and *Shank3* KO mice) to treatment administration (Fig. 4C). Solely considering the *Oxt* and *Oxtr* markers, we pinpointed cluster 1, consisting of *Fmr1* KO and *Shank3* KO mice with low levels of *Oxt* and *Oxtr*, suggesting a potential positive response to oxytocin treatment in this subgroup.

In conclusion, this study showed the first successful proof-of-concept for the stratification of four mouse models using five molecular markers.

DISCUSSION

Our findings elucidate distinct dynamics in the expression patterns of the two mRNA families across five brain structures in response to two types of social interactions in WT mice. Notably, SI mate elicited a sustained pattern of expression, unlike NSI object, which displayed a rapid and transient increase, indicating a response to the novelty of the environment, or no response. SI unknown exhibited a unique pattern within 45 min, setting it apart from the other two stimuli. Furthermore, our results suggest a distinct molecular mechanism of activation for each social interaction in these five structures. SI unknown predominantly impacts the OT family in the CPU, NAC and PVN, as well as the IEG family in the PVN, SON and PFC. Conversely, SI mate primarily influences the OT family in the PVN, along with the IEG family in the PFC. While previous studies have highlighted the role of the CPU in facilitating mate interactions as a habitual behavior, and the NAC in orchestrating responses to SI unknown [33], our results reveal a more intricate and nuanced molecular mechanism across these structures.

Surprisingly, our findings unveiled a remarkably high positive correlation between *Oxt* and *Avp* mRNA levels in both WT mice and mouse models. *Oxt* and *Avp*, being paralog genes, are located only 11 kbp apart from each other (4 kbp in humans). Despite the identification of specific elements in this intergenic region in vitro that potentially promote neuron specificity [79], our results suggest that both mRNAs undergo similar regulation, and common regulatory elements may have been evolutionarily conserved. The robust correlation observed between *Oxt* and *Avp* mRNAs emphasizes the importance of considering both peptides in research studies.

Within the OT system, our results revealed distinct molecular dysregulations in each mouse model. Particularly, levels of *Oxt* and *Avp* mRNAs, as well as *Oxtr* across the structures delineated the four mouse models. Noteworthy, *Shank3* KO mice exhibited *Cd38* downregulation in the PFC and NAC. Given its association with social memory and recognition impairments [80], and the social novelty phenotype displayed by *Shank3* KO mice, our results position *Cd38* as a potential marker of social memory-related conditions. In contrast to the OT family, our results underscore widespread IEG dysregulations across brain structures in all four models, confirming synaptic plasticity impairment as a major hallmark of ASD. Notably, *Egr1*, *Foxp1* and *Homer1a* emerge as the most robust markers of social interactions in WT animals and the most dysregulated IEGs in the four models. These findings align with their previous association with ASD in both individuals with autism and mouse models mimicking the condition [56, 81–85].

IEG or OT at the protein/peptide level did not substantiate these findings, except c-Fos/*Fos* in the PVN of *Shank3* KO mice. Indeed, protein and mRNA involve distinct cellular processes, translation and transcription, and dynamics [75, 86]. This is particularly evident for IEGs that are highly regulated and responsive to the environment and stimuli. Indeed, as observed for FoxP1/*Foxp1* in the CPU of *Fmr1* KO mice, mRNAs are rapidly translated and degraded upon translation while protein levels are increased. For the OT family, we observed that *Oxt* transcription is relatively stable over several hours in the PVN of WT mice. In contrast, OT peptide levels are released in the plasma and brain within min upon activation of OT neurons in response to social, and non-social contexts, including stressful conditions (here, mouse handling and euthanasia) [31, 87–91], pointing to distinct mechanisms and dynamics governing peptide release and mRNA regulations. Notably, brain *Oxt* mRNAs, similar to OT peptide concentration [92], did not correlate with peripheral OT levels. However, levels of IEGs in accessible fluids, such as blood or cerebrospinal fluid, could be linked to autism, as shown by elevated Arc proteins in the blood of children with ASD [54]. Unlike OT peptide, which can be degraded and still detected through OT dosage [93, 94], our findings suggest *Oxt* or *Avp* mRNAs might be reliable markers for long-term synaptic plasticity in OT neurons.

Our results revealed robust impairments in social interaction with an unknown conspecific in *Fmr1* and *Shank3* KO mice, accompanied by pronounced motor stereotypies in *Shank3* KO mice, aligning with previous reports [95, 96]. Conversely, *Oprm1* KO and chronically isolated mice did not exhibit the expected social impairments [74, 76]. Their phenotype may have been influenced by the experimenter's sex [97], predominantly females in this study, as well as by experimental conditions designed to reduce animal stress. Indeed, a slight increase in light induced social impairments in *Oprm1* KO mice. Recently, it has been proposed that housing conditions and the duration of social isolation may interfere with social impairments previously observed in chronically isolated animals [62, 98]. Interestingly, none of the mouse models exhibited impaired social interaction with a cage mate, aligning with reports suggesting that interactions within the family environment were more manageable for children with ASD [99]. Notably, the stratification of the models using the five molecular markers—*Egr1*, *Foxp1*, *Homer1a*, *Oxt*, and *Oxtr*—consistently aligned with behavioral data. This analysis accurately predicted the molecular underpinnings of the observed behavioral differences between *Oprm1* KO and isolated mice and the other two models, as well as *Arc* KO mice. Despite their distinct profiles, it unveiled shared dysregulations in both *Fmr1* and *Shank3* KO mice, providing valuable insights into potential links with their respective social phenotypes and responsiveness to treatments.

In conclusion, our study offers valuable insights into the dynamics of OT and IEG mRNAs in WT animals and their dysregulations in mouse models displaying autism-like behaviors across five structures within the social circuit. Our findings not only enable the stratification of the four mouse models, but also allow the identification of subgroups within these models. Transcriptomic studies of postmortem brains from individuals with ASD have also identified dysregulations in *EGR1*, *CFOS*, *JUN*, *FOXP1*, *OXT*, and *OXTR* mRNAs [16–19], underscoring the relevance of this study to understanding the human condition. The stratification of other mouse models, such as *Cntnap2*, *Magel2*, or *Oxtr* KO mice [100–102], and different species, including *Shank3* KO rats [103], would enhance the predictive value of the five molecular markers in individuals affected by autism. Exploring additional structures within this circuit, such as the amygdala and lateral septum, could further contribute to the stratification of the models. Nevertheless, future research employing omic approaches beyond the oxytocin and synaptic plasticity families is essential to identify more molecular markers and potentially uncover novel therapeutic targets. This study represents the first proof-of-concept for molecular stratification using brain tissues of mouse models, with the aim of improving the success of clinical trials and personalized treatment for ASD. Additionally, our work may offer the potential for more precise and faster ASD diagnostics, complementing behavioral screenings [2].

DATA AVAILABILITY

All the raw, mean and statistical data are available in supplementary Tables. All R language analyses and codes (https://doi.org/10.57745/AH9UWC), along with full western blot gels (https://doi.org/10.25493/33R2-6YN), have been uploaded in the French academic data.gouv.fr repository. Movies of behavioral experiments are available upon request.

REFERENCES

1. Lord C, Brugha TS, Charman T, Cusack J, Dumas G, Frazier T, et al. Autism spectrum disorder. Nat Rev Dis Primers. 2020;6:5.
2. American Psychiatric Association. Diagnostic and statistical manual of mental disorders. 5th ed. American Psychiatric Association; 2013.
3. Kaufmann WE, Kidd SA, Andrews HF, Budimirovic DB, Esler A, Haas-Givler B, et al. Autism spectrum disorder in fragile X syndrome: cooccurring conditions and current treatment. Pediatrics. 2017;139:S194–S206.
4. Asta L, Persico AM. Differential predictors of response to early start Denver model vs. early intensive behavioral intervention in young children with autism spectrum disorder: a systematic review and meta-analysis. Brain Sci. 2022;12:1499.
5. McCracken JT, McGough J, Shah B, Cronin P, Hong D, Aman MG, et al. Risperidone in children with autism and serious behavioral problems. N Engl J Med. 2002;347:314–21.
6. Owen R, Sikich L, Marcus RN, Corey-Lisle P, Manos G, McQuade RD, et al. Aripiprazole in the treatment of irritability in children and adolescents with autistic disorder. Pediatrics. 2009;124:1533–40.
7. Martins D, Paduraru M, Paloyelis Y. Heterogeneity in response to repeated intranasal oxytocin in schizophrenia and autism spectrum disorders: a meta-analysis of variance. Br J Pharmacol. 2022;179:1525–43.
8. Annamneedi A, Gora C, Dudas A, Leray X, Bozon V, Crépieux P, et al. Towards the convergent therapeutic potential of G protein-coupled receptors in autism spectrum disorders. Br J Pharmacol 2023;bph.16216.
9. Foss-Feig JH, Adkinson BD, Ji JL, Yang G, Srihari VH, McPartland JC, et al. Searching for cross-diagnostic convergence: neural mechanisms governing excitation and inhibition balance in schizophrenia and autism spectrum disorders. Biol Psychiatry. 2017;81:848–61.
10. Fetit R, Hillary RF, Price DJ, Lawrie SM. The neuropathology of autism: a systematic review of post-mortem studies of autism and related disorders. Neurosci Biobehav Rev. 2021;129:35–62.
11. Green JJ, Hollander E. Autism and oxytocin: new developments in translational approaches to therapeutics. Neurotherapeutics. 2010;7:250–7.
12. Moerkerke M, Peeters M, de Vries L, Daniels N, Steyaert J, Alaerts K, et al. Endogenous oxytocin levels in autism—a meta-analysis. Brain Sci. 2021;11:1545.
13. Gandal MJ, Haney JR, Wamsley B, Yap CX, Parhami S, Emani PS, et al. Broad transcriptomic dysregulation occurs across the cerebral cortex in ASD. Nature. 2022;611:532–9.
14. Autism Spectrum Disorders Working Group of The Psychiatric Genomics Consortium. Meta-analysis of GWAS of over 16,000 individuals with autism spectrum disorder highlights a novel locus at 10q24.32 and a significant overlap with schizophrenia. Mol Autism. 2017;8:21.
15. LoParo D, Waldman ID. The oxytocin receptor gene (OXTR) is associated with autism spectrum disorder: a meta-analysis. Mol Psychiatry. 2015;20:640–6.
16. Satterstrom FK, Kosmicki JA, Wang J, Breen MS, De Rubeis S, An J-Y, et al. Large-scale exome sequencing study implicates both developmental and functional changes in the neurobiology of autism. Cell. 2020;180:568–84.e23.
17. Gandal MJ, Zhang P, Hadjimichael E, Walker RL, Chen C, Liu S, et al. Transcriptome-wide isoform-level dysregulation in ASD, schizophrenia, and bipolar disorder. Science. 2018;362:eaat8127.
18. Wamsley B, Bicks L, Cheng Y, Kawaguchi R, Quintero D, Margolis M, et al. Molecular cascades and cell type-specific signatures in ASD revealed by single-cell genomics. Science. 2024;384:eadh2602.
19. Parras A, Anta H, Santos-Galindo M, Swarup V, Elorza A, Nieto-González JL, et al. Autism-like phenotype and risk gene mRNA deadenylation by CPEB4 mis-splicing. Nature. 2018;560:441–6.
20. Insel TR. The challenge of translation in social neuroscience: a review of oxytocin, vasopressin, and affiliative behavior. Neuron. 2010;65:768–79.
21. Quintana DS, Rokicki J, van der Meer D, Alnæs D, Kaufmann T, Córdova-Palomera A, et al. Oxytocin pathway gene networks in the human brain. Nat Commun. 2019;10:668.
22. Menon R, Neumann ID. Detection, processing and reinforcement of social cues: regulation by the oxytocin system. Nat Rev Neurosci. 2023;24:761–77.
23. Donaldson ZR, Young LJ. Oxytocin, vasopressin, and the neurogenetics of sociality. Science. 2008;322:900–4.
24. Madrigal MP, Jurado S. Specification of oxytocinergic and vasopressinergic circuits in the developing mouse brain. Commun Biol. 2021;4:586.
25. Soumier A, Habart M, Lio G, Demily C, Sirigu A. Differential fate between oxytocin and vasopressin cells in the developing mouse brain. iScience. 2022;25:103655.
26. Son S, Manjila SB, Newmaster KT, Wu Y, Vanselow DJ, Ciarletta M, et al. Whole-brain wiring diagram of oxytocin system in adult mice. J Neurosci. 2022;42:5021–33.
27. Liao P-Y, Chiu Y-M, Yu J-H, Chen S-K. Mapping central projection of oxytocin neurons in unmated mice using cre and alkaline phosphatase reporter. Front Neuroanat. 2020;14:559402.
28. Newmaster KT, Nolan ZT, Chon U, Vanselow DJ, Weit AR, Tabbaa M, et al. Quantitative cellular-resolution map of the oxytocin receptor in postnatally developing mouse brains. Nat Commun. 2020;11:1885.
29. Grinevich V, Knobloch-Bollmann HS, Eliava M, Busnelli M, Chini B. Assembling the puzzle: pathways of oxytocin signaling in the brain. Biol Psychiatry. 2016;79:155–64.
30. Grinevich V, Ludwig M. The multiple faces of the oxytocin and vasopressin systems in the brain. J Neuroendocrinol. 2021;33:e13004.
31. Grinevich V, Neumann ID. Brain oxytocin: how puzzle stones from animal studies translate into psychiatry. Mol Psychiatry. 2021;26:265–79.
32. Peça J, Feliciano C, Ting JT, Wang W, Wells MF, Venkatraman TN, et al. Shank3 mutant mice display autistic-like behaviours and striatal dysfunction. Nature. 2011;472:437–42.
33. Dölen G, Darvishzadeh A, Huang KW, Malenka RC. Social reward requires coordinated activity of nucleus accumbens oxytocin and serotonin. Nature. 2013;501:179–84.
34. Vollweiter D, Shergill JK, Hilse A, Kochlamazashvili G, Koch SP, Mueller S, et al. Intersectin deficiency impairs cortico-striatal neurotransmission and causes obsessive-compulsive behaviors in mice. Proc Natl Acad Sci USA. 2023;120:e2304323120.
35. Augustine F, Nebel MB, Mostofsky SH, Mahone EM, Singer HS. Aberrant prefrontal cortical-striatal functional connectivity in children with primary complex motor stereotypies. Cortex. 2021;142:272–82.
36. Meyer-Lindenberg A, Domes G, Kirsch P, Heinrichs M. Oxytocin and vasopressin in the human brain: social neuropeptides for translational medicine. Nat Rev Neurosci. 2011;12:524–38.
37. Rae M, Lemos Duarte M, Gomes I, Camarini R, Devi LA. Oxytocin and vasopressin: signalling, behavioural modulation and potential therapeutic effects. Br J Pharmacol. 2022;179:1544–64.
38. Borie AM, Theofanopoulou C, Andari E. The promiscuity of the oxytocin-vasopressin systems and their involvement in autism spectrum disorder. Handb Clin Neurol. 2021;182:121–40.
39. Peñagarikano O. Oxytocin in animal models of autism spectrum disorder. Dev Neurobiol. 2017;77:202–13.
40. Freeman SM, Palumbo MC, Lawrence RH, Smith AL, Goodman MM, Bales KL. Effect of age and autism spectrum disorder on oxytocin receptor density in the human basal forebrain and midbrain. Transl Psychiatry. 2018;8:257.
41. Uhrig S, Hirth N, Broccoli L, von Wilmsdorff M, Bauer M, Sommer C, et al. Reduced oxytocin receptor gene expression and binding sites in different brain regions in schizophrenia: a post-mortem study. Schizophr Res. 2016;177:59–66.
42. Pujol CN, Pellissier LP, Clément C, Becker JAJ, Le Merrer J. Back-translating behavioral intervention for autism spectrum disorders to mice with blunted reward restores social abilities. Transl Psychiatry. 2018;8:197.
43. Tabak BA, Teed AR, Castle E, Dutcher JM, Meyer ML, Bryan R, et al. Null results of oxytocin and vasopressin administration across a range of social cognitive and behavioral paradigms: Evidence from a randomized controlled trial. Psychoneuroendocrinology. 2019;107:124–32.
44. Sikich L, Kolevzon A, King BH, McDougle CJ, Sanders KB, Kim S-J, et al. Intranasal oxytocin in children and adolescents with autism spectrum disorder. N Engl J Med. 2021;385:1462–73.
45. Parker KJ, Oztan O, Libove RA, Sumiyoshi RD, Jackson LP, Karhson DS, et al. Intranasal oxytocin treatment for social deficits and biomarkers of response in children with autism. Proc Natl Acad Sci USA. 2017;114:8119–24.
46. Montanari M, Martella G, Bonsi P, Meringolo M. Autism spectrum disorder: focus on glutamatergic neurotransmission. Int J Mol Sci. 2022;23:3861.
47. El-Ansary A, Al-Ayadhi L. GABAergic/glutamatergic imbalance relative to excessive neuroinflammation in autism spectrum disorders. J Neuroinflamm. 2014;11:189.
48. Froemke RC, Young LJ. Oxytocin, neural plasticity, and social behavior. Annu Rev Neurosci. 2021;44:359–81.
49. Gur R, Tendler A, Wagner S. Long-term social recognition memory is mediated by oxytocin-dependent synaptic plasticity in the medial amygdala. Biol Psychiatry. 2014;76:377–86.
50. Cardoso SD, Teles MC, Oliveira RF. Neurogenomic mechanisms of social plasticity. J Exp Biol. 2015;218:140–9.
51. Chien W-H, Gau SS-F, Chen C-H, Tsai W-C, Wu Y-Y, Chen P-H, et al. Increased gene expression of FOXP1 in patients with autism spectrum disorders. Mol Autism. 2013;4:23.

52. Saghazadeh A, Rezaei N. Brain-derived neurotrophic factor levels in autism: a systematic review and meta-analysis. J Autism Dev Disord. 2017;47:1018–29.
53. Tomaiuolo P, Piras IS, Sain SB, Picinelli C, Baccarin M, Castronovo P, et al. RNA sequencing of blood from sex- and age-matched discordant siblings supports immune and transcriptional dysregulation in autism spectrum disorder. Sci Rep. 2023;13:807.
54. Alhowikan AM. Activity-regulated cytoskeleton-associated protein dysfunction may contribute to memory disorder and earlier detection of autism spectrum disorders. Med Princ Pract. 2016;25:350–4.
55. Zhang P, Omanska A, Ander BP, Gandal MJ, Stamova B, Schumann CM. Neuron-specific transcriptomic signatures indicate neuroinflammation and altered neuronal activity in ASD temporal cortex. Proc Natl Acad Sci USA. 2023;120:e2206758120.
56. Banerjee A, Luong JA, Ho A, Saib AO, Ploski JE. Overexpression of Homer1a in the basal and lateral amygdala impairs fear conditioning and induces an autism-like social impairment. Mol Autism. 2016;7:16.
57. Schmit TL, Dowell JA, Maes ME, Wilhelm M. c-Jun N-terminal kinase regulates mGluR-dependent expression of post-synaptic FMRP target proteins. J Neurochem. 2013;127:772–81.
58. Niere F, Wilkerson JR, Huber KM. Evidence for a fragile X mental retardation protein-mediated translational switch in metabotropic glutamate receptor-triggered Arc translation and long-term depression. J Neurosci. 2012;32:5924–36.
59. Matthes HW, Maldonado R, Simonin F, Valverde O, Slowe S, Kitchen I, et al. Loss of morphine-induced analgesia, reward effect and withdrawal symptoms in mice lacking the mu-opioid-receptor gene. Nature. 1996;383:819–23.
60. Mientjes EJ, Nieuwenhuizen I, Kirkpatrick L, Zu T, Hoogeveen-Westerveld M, Severijnen L, et al. The generation of a conditional Fmr1 knock out mouse model to study Fmrp function in vivo. Neurobiol Dis. 2006;21:549–55.
61. Wang KH, Majewska A, Schummers J, Farley B, Hu C, Sur M, et al. In vivo two-photon imaging reveals a role of arc in enhancing orientation specificity in visual cortex. Cell. 2006;126:389–402.
62. Pellissier L, Gora C, Dudas A, Court L, Annamneedi A, Lefort G, et al. Effect of the social environment on olfaction and social skills in WT and a mouse model of autism. 2024. https://doi.org/10.21203/rs.3.rs-3759429/v1.
63. Roullet FI, Crawley JN. Mouse models of autism: testing hypotheses about molecular mechanisms. Curr Top Behav Neurosci. 2011;7:187–212.
64. Kilkenny C, Browne WJ, Cuthill IC, Emerson M, Altman DG. Improving bioscience research reporting: the ARRIVE guidelines for reporting animal research. PLoS Biol. 2010;8:e1000412.
65. R Core Team. R: a language and environment for statistical computing. 2017. https://www.R-project.org/.
66. Lê S, Josse J, Husson F. FactoMineR: an R package for multivariate analysis. J Stat Soft 2008;25. https://doi.org/10.18637/jss.v025.i01.
67. Leek JT, Johnson WE, Parker HS, Jaffe AE, Storey JD. The sva package for removing batch effects and other unwanted variation in high-throughput experiments. Bioinformatics. 2012;28:882–3.
68. Kassambara A. rstatix: pipe-friendly framework for basic statistical tests. 2023. https://CRAN.R-project.org/package=rstatix.
69. Benjamini Y, Hochberg Y. Controlling the false discovery rate: a practical and powerful approach to multiple testing. J R Stat Soc: Ser B (Methodol). 1995;57:289–300.
70. Russell VL. emmeans: estimated marginal means, aka least-squares means. 2023. https://CRAN.R-project.org/package=emmeans.
71. Singh A, Shannon CP, Gautier B, Rohart F, Vacher M, Tebbutt SJ, et al. DIABLO: an integrative approach for identifying key molecular drivers from multi-omics assays. Bioinformatics. 2019;35:3055–62.
72. Rohart F, Gautier B, Singh A, Lê Cao K-A. mixOmics: an R package for 'omics feature selection and multiple data integration. PLoS Comput Biol. 2017;13:e1005752.
73. Venables WN, Ripley BD. Modern applied statistics with S. 4th ed. New York: Springer; 2002.
74. Becker JAJ, Clesse D, Spiegelhalter C, Schwab Y, Le Merrer J, Kieffer BL. Autistic-like syndrome in mu opioid receptor null mice is relieved by facilitated mGluR4 activity. Neuropsychopharmacology. 2014;39:2049–60.
75. Kat R, Arroyo-Araujo M, de Vries RBM, Koopmans MA, de Boer SF, Kas MJH. Translational validity and methodological underreporting in animal research: a systematic review and meta-analysis of the Fragile X syndrome (Fmr1 KO) rodent model. Neurosci Biobehav Rev. 2022;139:104722.
76. Matsumoto K, Fujiwara H, Araki R, Yabe T. Post-weaning social isolation of mice: a putative animal model of developmental disorders. J Pharmacol Sci. 2019;141:111–8.
77. Wang T, Zhao T, Liu L, Teng H, Fan T, Li Y, et al. Integrative analysis prioritised oxytocin-related biomarkers associated with the aetiology of autism spectrum disorder. EBioMedicine. 2022;81:104091.
78. Managò F, Mereu M, Mastwal S, Mastrogiacomo R, Scheggia D, Emanuele M, et al. Genetic disruption of Arc/Arg3.1 in mice causes alterations in dopamine and neurobehavioral phenotypes related to schizophrenia. Cell Rep. 2016;16:2116–28.
79. Fields RL, House SB, Gainer H. Regulatory domains in the intergenic region of the oxytocin and vasopressin genes that control their hypothalamus-specific expression in vitro. J Neurosci. 2003;23:7801–9.
80. Jin D, Liu H-X, Hirai H, Torashima T, Nagai T, Lopatina O, et al. CD38 is critical for social behaviour by regulating oxytocin secretion. Nature. 2007;446:41–45.
81. Liu X, Han D, Somel M, Jiang X, Hu H, Guijarro P, et al. Disruption of an evolutionarily novel synaptic expression pattern in autism. PLoS Biol. 2016;14:e1002558.
82. Bacon C, Schneider M, Le Magueresse C, Froehlich H, Sticht C, Gluch C, et al. Brain-specific Foxp1 deletion impairs neuronal development and causes autistic-like behaviour. Mol Psychiatry. 2015;20:632–9.
83. Jaubert PJ, Golub MS, Lo YY, Germann SL, Dehoff MH, Worley PF, et al. Complex, multimodal behavioral profile of the Homer1 knockout mouse. Genes Brain Behav. 2007;6:141–54.
84. Trelles MP, Levy T, Lerman B, Siper P, Lozano R, Halpern D, et al. Individuals with FOXP1 syndrome present with a complex neurobehavioral profile with high rates of ADHD, anxiety, repetitive behaviors, and sensory symptoms. Mol Autism. 2021;12:61.
85. Feliciano P, Zhou X, Astrovskaya I, Turner TN, Wang T, Brueggeman L, et al. Exome sequencing of 457 autism families recruited online provides evidence for autism risk genes. NPJ Genom Med. 2019;4:19.
86. Wagle S, Kraynyukova N, Hafner A-S, Tchumatchenko T. Computational insights into mRNA and protein dynamics underlying synaptic plasticity rules. Mol Cell Neurosci. 2023;125:103846.
87. Neumann I, Landgraf R. Septal and hippocampal release of oxytocin, but not vasopressin, in the conscious lactating rat during suckling. J Neuroendocrinol. 1989;1:305–8.
88. Neumann I, Ludwig M, Engelmann M, Pittman QJ, Landgraf R. Simultaneous microdialysis in blood and brain: oxytocin and vasopressin release in response to central and peripheral osmotic stimulation and suckling in the rat. Neuroendocrinology. 1993;58:637–45.
89. Veenema AH, Neumann ID. Central vasopressin and oxytocin release: regulation of complex social behaviours. Prog Brain Res. 2008;170:261–76.
90. Schneiderman I, Zagoory-Sharon O, Leckman JF, Feldman R. Oxytocin during the initial stages of romantic attachment: relations to couples' interactive reciprocity. Psychoneuroendocrinology. 2012;37:1277–85.
91. Lukas M, Toth I, Veenema AH, Neumann ID. Oxytocin mediates rodent social memory within the lateral septum and the medial amygdala depending on the relevance of the social stimulus: male juvenile versus female adult conspecifics. Psychoneuroendocrinology. 2013;38:916–26.
92. Valstad M, Alvares GA, Egknud M, Matziorinis AM, Andreassen OA, Westlye LT, et al. The correlation between central and peripheral oxytocin concentrations: a systematic review and meta-analysis. Neurosci Biobehav Rev. 2017;78:117–24.
93. Rutigliano G, Rocchetti M, Paloyelis Y, Gilleen J, Sardella A, Cappucciati M, et al. Peripheral oxytocin and vasopressin: biomarkers of psychiatric disorders? A comprehensive systematic review and preliminary meta-analysis. Psychiatry Res. 2016;241:207–20.
94. Szeto A, McCabe PM, Nation DA, Tabak BA, Rossetti MA, McCullough ME, et al. Evaluation of enzyme immunoassay and radioimmunoassay methods for the measurement of plasma oxytocin. Psychosom Med. 2011;73:393–400.
95. Mei Y, Monteiro P, Zhou Y, Kim J-A, Gao X, Fu Z, et al. Adult restoration of Shank3 expression rescues selective autistic-like phenotypes. Nature. 2016;530:481–4.
96. Mineur YS, Huynh LX, Crusio WE. Social behavior deficits in the Fmr1 mutant mouse. Behav Brain Res. 2006;168:172–5.
97. Georgiou P, Zanos P, Mou T-CM, An X, Gerhard DM, Dryanovski DI, et al. Experimenters' sex modulates mouse behaviors and neural responses to ketamine via corticotropin releasing factor. Nat Neurosci. 2022;25:1191–1200.
98. Padilla-Coreano N, Tye KM, Zelikowsky M. Dynamic influences on the neural encoding of social valence. Nat Rev Neurosci. 2022;23:535–50.
99. Slaughter V, Ong SS. Social behaviors increase more when children with ASD are imitated by their mother vs. an unfamiliar adult. Autism Res. 2014;7:582–9.
100. Peñagarikano O, Abrahams BS, Herman EI, Winden KD, Gdalyahu A, Dong H, et al. Absence of CNTNAP2 leads to epilepsy, neuronal migration abnormalities, and core autism-related deficits. Cell. 2011;147:235–46.
101. Sala M, Braida D, Lentini D, Busnelli M, Bulgheroni E, Capurro V, et al. Pharmacologic rescue of impaired cognitive flexibility, social deficits, increased aggression, and seizure susceptibility in oxytocin receptor null mice: a neurobehavioral model of autism. Biol Psychiatry. 2011;69:875–82.
102. Meziane H, Schaller F, Bauer S, Villard C, Matarazzo V, Riet F, et al. An early postnatal oxytocin treatment prevents social and learning deficits in adult mice deficient for Magel2, a gene involved in Prader–Willi syndrome and autism. Biol Psychiatry. 2015;78:85–94.

103. Jacot-Descombes S, Keshav NU, Dickstein DL, Wicinski B, Janssen WGM, Hiester LL, et al. Altered synaptic ultrastructure in the prefrontal cortex of Shank3-deficient rats. Mol Autism. 2020;11:89.

ACKNOWLEDGEMENTS

Mouse breeding and care were performed at the INRAE Animal Physiology Facility (https://doi.org/10.15454/1.5573896321728955E12). This work has benefited from the facilities and expertise of the "Informatique Scientifique Locale et Analyses de Données" (ISLANDe) of the UMR PRC, INRAE. We used ChatGPT, developed by OpenAI, for assistance with English editing. We thank Dr. E. Valjent, Dr. R. Yvinec, Dr. P. Crepieux, Dr. P. Chamero, Dr. A. Carvalho, and Dr. J. Collet for their advice on the manuscript. This project has received funding from the European Research Council (ERC) under the European Union's Horizon 2020 research and innovation program (grant agreement No. 851231). This work was supported by the INRAE "SOCIALOME" project (PAF_29). LPP, CG, and AD acknowledge the LabEx MabImprove (grant ANR-10-LABX-53-01) for the financial support of CG and AD PhD's co-fund.

AUTHOR CONTRIBUTIONS

CG, AD, OV, LD, EP, and LP designed and performed the experiments; CG, AD, OV, LD, EP, and LP contributed to the data collection; CG, AD, OV, LD, GL, and LP contributed to the interpretation of data; GL performed all statistical analysis, data modeling, and integration; CG, GL, and LP wrote the original drafts; CG, AD, OV, LD, EP, GL, and LP reviewed and edited the manuscript; LP contributed to the funding acquisition, project conceptualization and supervision.

COMPETING INTERESTS

The authors declare no competing interests.

ADDITIONAL INFORMATION

Supplementary information The online version contains supplementary material available at https://doi.org/10.1038/s41398-024-03113-5.

Correspondence and requests for materials should be addressed to Lucie P. Pellissier.